Available online at www.sciencedirect.com
SCIENCE DIRECT®
ELSEVIER
Nuclear Instruments and Methods in Physics Research B 206 (2003) 846–850
NIM B
Beam Interactions with Materials & Atoms
www.elsevier.com/locate/nimb

Crater formation and sputtering by cluster impacts

Z. Insepov [a,*], L.P. Allen [b], C. Santeufemio [b], K.S. Jones [c], I. Yamada [a,d]

[a] LASTI, Himeji Institute of Technology, 3-1-2 Kouto, Kamigori, Ako, Hyogo 678-1205, Japan
[b] Epion Corporation, 37 Manning Road, Billerica, MA 01821, USA
[c] Department of Materials Science and Engineering, University of Florida, Gainesville, FL 32611, USA
[d] Collaborative Research Center for Cluster Ion Beam Process Technology, Japan

Abstract

A multiscale computational model coupling atomistic molecular dynamics simulations with continuum elasticity was used for studying craters formed on Si surfaces by Ar cluster impacts, with energies of 20–50 eV/atom. The results were confirmed by atomic force microscopy/transmission electron microscopy. They show that on a Si (1 0 0), craters are nearly triangular in cross-section, with the facets directed along the close-packed (1 1 1) planes, and exhibit fourfold symmetry. The craters on Si (1 1 1) surface are well rounded in cross-section and the top-view shows a complicated sixfold or triangular image. The sputtering yield from Si surfaces bombarded with B_{10} cluster ions, with energy of 1–15 keV, was calculated.

PACS: 36.40; 61.43.B; 34.50.D; 82.65.P; 96.20.K; 61.72.T
Keywords: Multiscale; Cluster; Crater; AFM; TEM; Decaborane

1. Introduction

Interactions of energetic clusters of atoms with solid surfaces demonstrate unique phenomena and promise new applications for surface modification technology [1–6]. Large Ar clusters, with energy up to 20 keV are used for surface etching and smoothing.

Decaborane cluster ion ($B_{10}H_{14}$) implantation is of a high interest for the silicon industry as it gives an alternative method for fabricating very shallow p–n junction for future devices [7–9]. Unfortunately, both the theory and experiments of decaborane implantation into silicon are sparse.

The main surface modification phenomenon for gas cluster ion beam (GCIB) technology is the surface smoothing effect. A crystal surface, with an initial average surface roughness of tens or hundreds of angstroms, becomes atomically flat, with the residual roughness of a few angstroms [5,7,8,11]. The GCIB smoothing typically occurs after irradiation by an ionized Ar_n ($n \sim 1000$–10 000) cluster beam at a charge fluence of 10^{14}–10^{16} ions/cm^2.

The aim of this work is to simulate individual Ar gas and Decaborane cluster impacts by a multiscale method and compare the results with high-resolution transmission electron microscopy

* Corresponding author. Tel.: +81-791-58-0412; fax: +81-791-58-0242.
E-mail address: insepov@lasti.himeji-tech.ac.jp (Z. Insepov).

0168-583X/03/$ - see front matter © 2003 Elsevier Science B.V. All rights reserved.
doi:10.1016/S0168-583X(03)00876-0

(HRTEM) and atomic force microscopy (AFM) experimental observation.

2. Simulation method

In our multiscale simulation method, molecular dynamics (MD) is utilized for the atoms in the central collision zone, and continuum mechanics and thermodynamics outside this zone. The details of the method could be found elsewhere [10,11].

Energetic cluster impacts create intense collisions between atoms in the central zone where equivalent temperature and pressure may reach 10^5 K and 10^3 GPa, respectively [5]. The problem of the boundary conditions for this case can be examined by considering shock waves created by the energetic cluster impact. Unphysical reflections of the shock waves from the system boundary may show up in MD results, distorting the picture of the investigated process. Shock wave reflections have been revealed for the systems as large as 4×10^5 target atoms studied by MD if fixed periodic boundary conditions (PBC) are used, for the cluster impact energy as low as 10 kV [12,13].

In MD, the Buckingham potential is used to represent two-body forces between cluster atoms and between the cluster and target atoms while interaction between Si atoms were represented by the Stillinger–Weber potential. The clusters used in simulations contained about 135–369 atoms and had kinetic energy of 25–100 eV/atom. The cylindrical target model contained $\sim 3 \times 10^5$ atoms in the central MD zone while the continuum mechanics calculations extended to 10 times larger volume.

Implantation of Decaborane ions, in the energy range of 1–15 keV, into Si and sputtering of the target was simulated. The Decaborane molecule was modeled as a B_{10} cluster. Based on the cluster energy and ion fluence, 10^{13}–10^{16} ion/cm^2, a target consisting of about 2×10^5 Si atoms was used. The ZBL potential at short distances combined with the Stillinger–Weber potential at equilibrium distances was used to evaluate interactions between two and three Si atoms, as usual [6]. Interaction between B and Si atoms was modeled via the ZBL screened Coulomb potential at short distances, $r < 0.52$ Å, and with a Morse-type potential at long distances, $r > 0.86$ Å. Interaction between two B dopants was modeled with an (exp-6)-type potential, with the depth of 0.2 eV and the equilibrium distance of 1.5 Å. Silicon atoms were considered as sputtered if they cross a plane $2R_{\text{cut}}$ above the surface and have positive normal velocity component, where R_{cut} is a distance of interaction cut, and the results were averaged for many B_{10} impacts.

Fig. 1 shows a side-view for the simulated crater formed by a 25 eV/atom Ar_{135} cluster impact on a Si (1 0 0) surface after the time intervals of 14.3 ps. This picture shows a nearly triangular facetting of the crater, which is due to higher lattice energy of the (1 1 1) plane.

The top-view of the crater is given in Fig. 2. It shows a nearly fourfold symmetry crater with facets formed by four (1 1 1) planes crossing the (1 0 0) surface. This figure shows a thin slice of the substrate parallel to surface made by cutting out the atoms with the positions within the interval: -3 Å $< z_i < 0.05$ Å (z-axis is perpendicular to the surface, and a negative value means an atom below the initial surface).

The Si (1 1 1) surface shows facetting features quite different from that of (1 0 0) surface as can be viewed in Figs. 3 and 4. We see that the side-view has a round-shaped crater and the top-view has a six-point shape, previously unobserved in simulation or in experiment. Four atomic layers from the

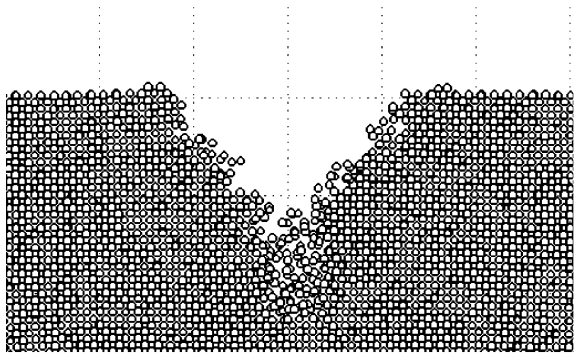

Fig. 1. MD result for the side-view of the crater formed on a Si (1 0 0) surface by a Ar_{135} cluster impact, and with energy of 24 eV/atom, 14.3 ps after the beginning of impact.

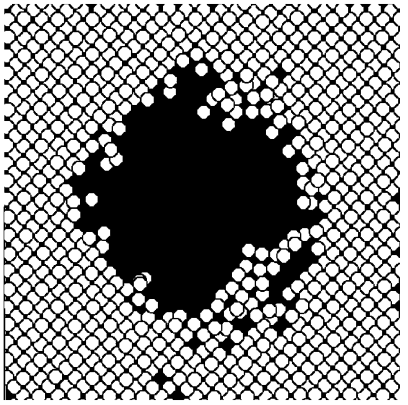

Fig. 2. Top-view of the crater formed by a Ar_{135}, 25 eV/atom, cluster impact on a Si (1 0 0) surface.

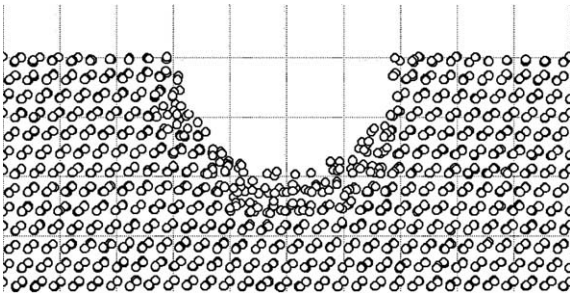

Fig. 3. MD result for the side-view of a crater formed on a Si (1 1 1) surface by a Ar_{135} cluster impact, with energy of 24 eV/atom, 14.4 ps after the beginning of impact.

top of non-irradiated surface are shown: -4 Å $< z_i < 0.05$ Å.

Fig. 5 presents the result of this simulation for the energy dependence of the total sputtering yield of Si (1 0 0) surface bombarded with B_{10} cluster ions at different energies in the 1–15 keV range. The experimental value of the sputtering yield, four sputtered Si atoms at 12 keV [9]. For energies above 10 keV, the MD data points and the experimental data point could be fitted with an empirical formula $Y = A\exp[-B/(E + C)]$ that was suggested for low-energy sputtering yield from metals bombarded with single ions [14]. Our calculations also show that of about 70% of the Boron atoms are reflected back into vacuum for

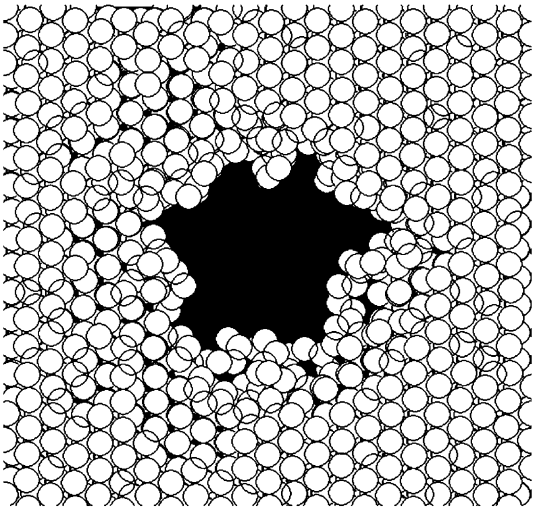

Fig. 4. Top-view of the crater formed on a Si (1 1 1) surface by an Ar_{135}, 25 eV/atom, cluster impact. The complicated faceting feature is clearly seen and may be compared with the AFM image of Fig. 7.

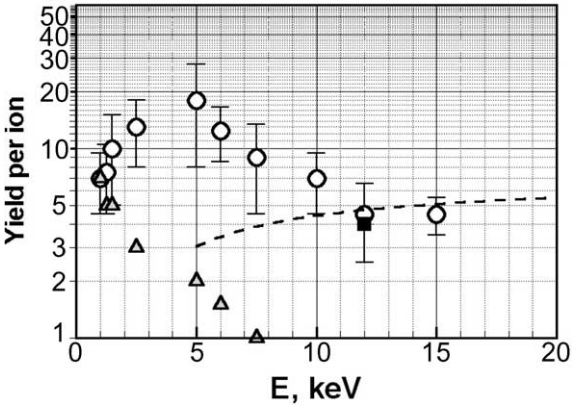

Fig. 5. Open circles: Si sputtering yield caused by B_{10} cluster implantations, with energies of 1–15 keV, calculated in this paper. Filled square: Experimental data point is for 12 keV. The dash line shows an empirical relation obtained for low energy sputtering yield of metals: $Y \sim A\exp[-B/(E + C)]$ [14] caused by single-ion bombardment. The following parameters: $A = 7$, $B = 5$, $C = 1$ were used for fitting. Triangles show the number of reflected boron atoms.

energies lower than 1.5 keV, and the reflection probability drops down fast for energies above 5 keV.

3. Experimental observation of cluster impact craters

Polished Si substrates with a native oxide were exposed to a low fluence, 10^{10} ions/cm^2, Ar and O_2 gas cluster ions using both 24 and 3 kV acceleration energies. TEM cross-section images and AFM images of the cluster impacts were studied. The images of individual gas cluster ion impacts were obtained using a JEOL 2010 TEM with a field-emission gun. Images were formed by orientation of the sample such that the transmitted beam was parallel to the $\langle 1\,1\,0\rangle$ direction of the lattice. Fig. 6 shows HRTEM cross-section of an individual Ar gas cluster ion crater formed by 24 kV acceleration into Si (1 0 0). The image cross-section shape agrees well with Fig. 1, showing a conical impact crater with the (1 1 1) planes aligned with the crater walls. The 24 kV individual impact crater images of an O_2 cluster into Si (1 1 1) is given in Fig. 7.

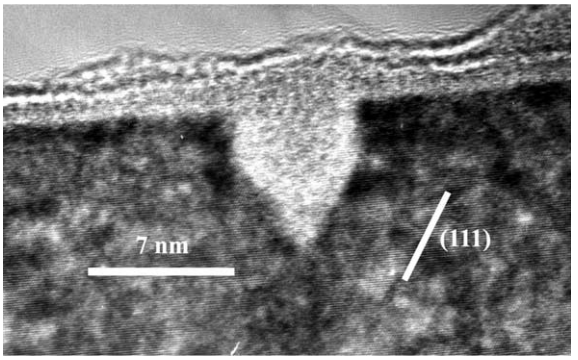

Fig. 6. HRTEM cross-section image of an individual 24 kV Ar cluster ion impact into Si (1 0 0). Crater conical edges align along the (1 1 1) lattice planes.

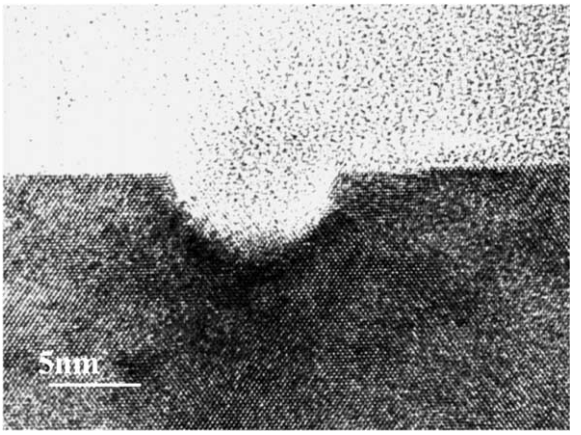

Fig. 7. HRTEM cross-section image of an individual 24 kV O_2 cluster ion impact into Si (1 1 1). Rounder impact craters typically resulted from the O_2 cluster process, perhaps from the immediate oxidation of the Si and the change in associated bond strength of the forming crater wall.

Fig. 8(a) and (b) show the surface view of individual hillocks as observed by 100 nm^2 AFM

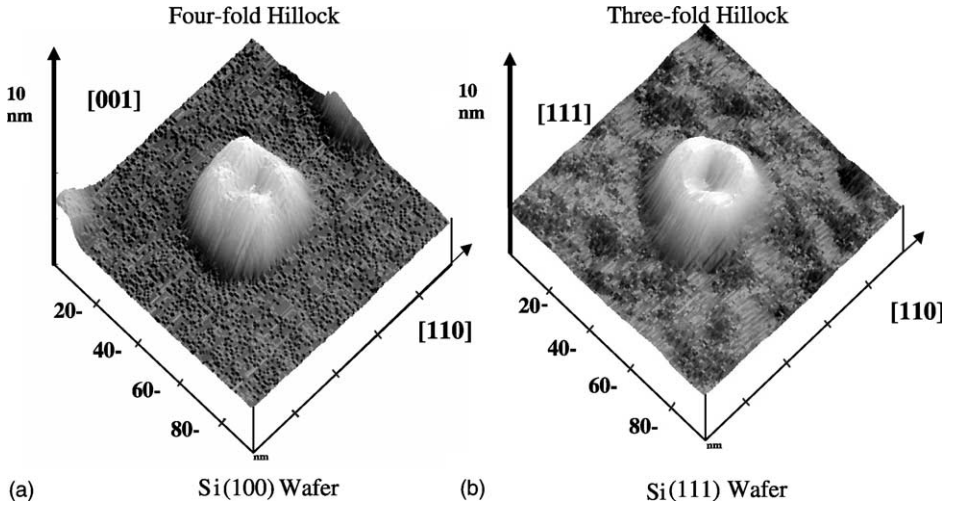

Fig. 8. Three-dimensional AFM image of fourfold symmetry of Si (1 0 0) 24 kV Ar cluster impact hillock (a) and threefold symmetry of Si (1 1 1) 24 kV Ar cluster impact hillock (b). Dimensions of both AFM images are 100 nm × 100 nm with a 10 nm height scaling.

scanned images. Fig. 8(a) shows the fourfold hillock symmetry formed over a 24 kV Ar gas cluster impact site, which reflects the atomic density the Si (1 0 0) substrate. Fig. 8(b) shows the threefold symmetry of the hillocks formed by a 24 kV Ar gas cluster impact into the Si (1 1 1) surface.

4. Conclusion

AFM and MD simulation of the craters and hillocks show and predict a fourfold symmetry for the 24 kV Ar GCIB individual impacts into Si (1 0 0) and a threefold (sixfold) symmetry for the 24 kV Ar GCIB individual impacts into Si (1 1 1). This is consistent with the density of atoms for the respective Si crystal orientations. The simulation of Decaborane implantation has revealed a clear surface effect. At low energy of 1–1.5 keV, most of boron atoms were reflected back into vacuum. More experiments should be done to confirm these findings.

Acknowledgements

The authors gratefully acknowledge valuable discussions with John Hautala, Tom Tetreault, Yan Shao, Mike Mack, and Allen Kirkpatrick of Epion Corporation. This work was partially supported by the NEDO project (Japan). The integral support of the USAF under contract #F33615-00-C-5404 is sincerely acknowledged. GCIB equipment and process work under DoC-NIST ATP award contract #70NANB8H4011 is also appreciated.

References

[1] J.-H. Song, S.N. Kwon, D.-K. Choi, W.-K. Choi, Nucl. Instr. and Meth. B 179 (2001) 568.
[2] L.P. Allen, K.S. Jones, C. Santeufemio, W. Brooks, D.B. Fenner, J. Hautala, in: Proceedings of the Near Surface Effects Conference, 5–10 August 2001, Kodiak Island, Alaska, Office of Naval Research, Arlington, VA, p. 16 (woodc@onr.navy.mil).
[3] P. von Blanckenhagen, A. Gruber, J. Gspann, Nucl. Instr. and Meth. B 122 (1997) 322.
[4] A. Gruber, J. Gspann, J. Vac. Sci. Technol. B 15 (6) (1997) 2362.
[5] I. Yamada, J. Matsuo, Z. Insepov, D. Takeuchi, M. Akizuki, N. Toyoda, J. Vac. Sci. Technol. A 14 (1996) 781.
[6] H. Hsieh, R.S. Averback, H. Sellers, C.P. Flynn, Phys. Rev. B 45 (1992) 4417.
[7] I. Yamada, J. Matsuo, Mater. Res. Soc. Symp. Proc. 396 (1996) 149.
[8] I. Yamada, J. Matsuo, Mater. Res. Soc. Symp. Proc. 427 (1996) 265.
[9] M. Sosnowski, M.A. Albano, C. Li, H.-J.L. Gossmann, D.C. Jacobson, Appl. Phys. Lett. 80 (2002) 592.
[10] Z. Insepov, M. Sosnowski, I. Yamada, Nucl. Instr. and Meth. B 127–128 (1997) 269.
[11] L.P. Allen, Z. Insepov, D.B. Fenner, C. Santeufemio, W. Brooks, K.S. Jones, I. Yamada, J. Appl. Phys. 92 (2002) 3671.
[12] Z. Insepov, I. Yamada, Nucl. Instr. and Meth. B 99 (1995) 248.
[13] M. Moseler, J. Nordiek, H. Haberland, Phys. Rev. B 56 (1997) 15439.
[14] T.G. Eck, L. Chen, private communication.